Extended Abstracts of the 1992 International Conference on Solid State Devices and Materials, Tsukuba, 1992, pp. 610-612

Threading Dislocation Reduction in InP/GaAs by Thin Strained Interlayer and Its Application to the Fabrication of 1.3 μm Wavelength Laser on GaAs

Yae OKUNO, Toshihiro KAWANO, Tomonobu TSUCHIYA, and Tsuyoshi TANIWATARI

Central Research Laboratory, Hitachi Ltd.

1-280 Higashi-koigakubo, Kokubunji-shi, Tokyo 185, Japan

This paper examines the reduction of threading dislocation by a thin strained interlayer (SIL), and long-wavelength lasers fabricated on a GaAs substrate with SILs. Cross-sectional transmission electron microscope (TEM) is used to observe the dislocation blocking ability of a InGaP SIL inserted in an InP layer grown on a GaAs substrate. The characteristics of the lasers are improved due to dislocation reduction. Their threshold current is reduced to 70% on average and is also distributed more uniformly.

1. INTRODUCTION

The fabrication of III-V devices on lattice-mismatched substrates is attractive because it is the key technology in developing OEICs (opto-electronic integrated circuits). There have been several attempts to make GaAs lasers on Si[1], InP lasers on Si[2,3], and InP lasers on GaAs[4]. One of the difficulties in these studies is how to reduce the dislocation density and suppress the degradation of the devices.

Inserting a strained layer superlattice (SLS)[5-9] is one of the conventional ways to reduce the dislocation density. It is assumed that dislocations are bent away by the strain field induced by the SLS at the lower interface[9]. Therefore, if a single strained interlayer (SIL) can provide the same strain field as an SLS does, it is expected to reduce the dislocation density as much as an SLS. In fact, dislocations are dramatically reduced by inserting a few monolayers of Si in a GaAs layer grown on a Si substrate[10]. However, this is thought to be due to the strong covalent Si-Si bonds. In this paper, we investigate the effect of an InGaP SIL on the InP/GaAs system. Its ability to reduce threading dislocations was observed by cross-sectional transmission electron microscope (TEM). Long-wavelength lasers were fabricated on a GaAs substrate using this technique. Their high performance proved the effect of SIL on crystal improvement.

2. EXPERIMENTAL

N-type GaAs (100) substrates were used throughout this research. They were cleaned with organic solvents and chemically etched in $4H_2SO_4:1H_2O_2:1H_2O$ solution, and loaded into the metalorganic chemical vapor deposition (MOCVD) reactor and heated to 600°C in an AsH_3 flow. Then InP was grown by conventional one-step growth. The growth pressure and growth rate were 40 torr and 40 nm/min. The dopant gases used for the growth of the laser structure were H_2Se or Si_2H_6 for n-type layers and DMZn for p-type layers.

Cross-sectional TEM was used to study the threading dislocation structure. The dislocation density of the top surface was estimated by counting etch pit patterns formed by a H_3PO_4/HBr etchant. The crystal quality was evaluated by X-ray diffraction (XRD) and photoluminescence (PL) spectra at room temperature. The thickness of the SILs was measured by CAT (composition analysis by thickness fringe) - TEM[11] observation.

3. DISLOCATION REDUCTION BY SIL

Figure 1 shows cross-sectional TEM views of the InP/GaAs samples with a (a) 50 Å (b) 25 Å thick $In_{0.65}Ga_{0.35}P$ SIL. According to the theory of Matthews and Blacklee[12], 25 Å equals the critical thickness of InGaP at this composition on InP. The total InP thickness was 3 µm and SILs were inserted 1 µm above the interface. It is obvious that 50 Å is thicker than optimum, so this SIL generates more dislocations than it blocks. 25 Å seems to be a suitable thickness because this SIL reduces dislocations effectively. It generates no extra misfit dislocations though it blocks fewer dislocations than the 50 Å SIL does. The dislocation density above the SIL is 60% of that below it. This is as much as SLS can acheive. However, this does not mean the 25 Å $In_{0.65}Ga_{0.35}P$ layer is the optimum SIL. More careful determination of both the optinum thickness and composition of the SIL is necessary to reduce dislocations more effectively.

4. LASER FABRICATION WITH SILs

Long-wavelength lasers emitting at 1.3 µm on a GaAs substrate were fabricated employing SILs (A). Figure 2 is a shematic diagram of the BH structure on InP/GaAs. Three SILs were embedded in the 5 µm n-InP buffer

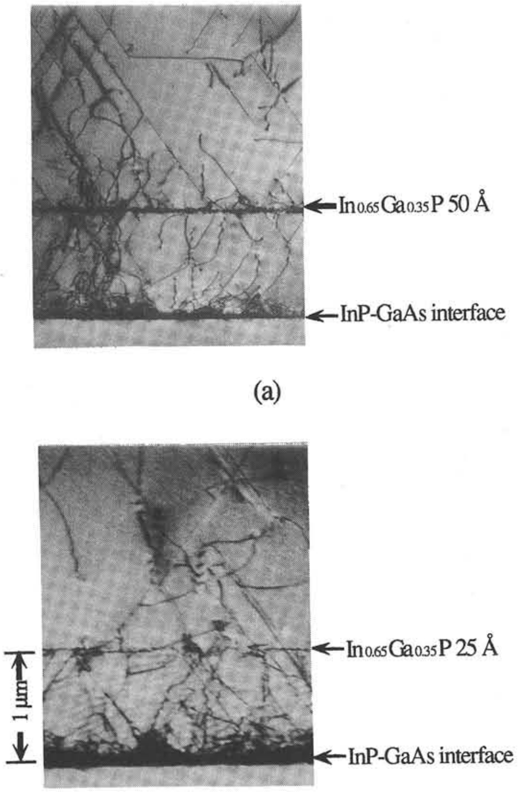

Figure 1 Cross-sectional TEM view of samples which comprise (a) 50 Å (b) 25 Å $In_{0.65}Ga_{0.35}P$ SIL

layer. One 25 Å $In_{0.65}Ga_{0.35}P$ layer was placed at 1 μm above the heterointerface, and two 30 Å $In_{0.89}Ga_{0.11}P$ layers were placed at 1.5 and 2 μm above the interface. The two $In_{0.89}Ga_{0.11}P$ SILs were expected to block dislocations which threaded through the bottom SIL, but they were thinner than we intended them to be. Thus, they should have no effect on dislocations. After the growth of this buffer layer, thermal cycle annealing (TCA) was performed by changing the substrate temperature between 750°C and 200°C 3 times. This annealing reduced the full width at half maximum of the XRD of buffer layer from 260 to 230 arcsec, and reduced the

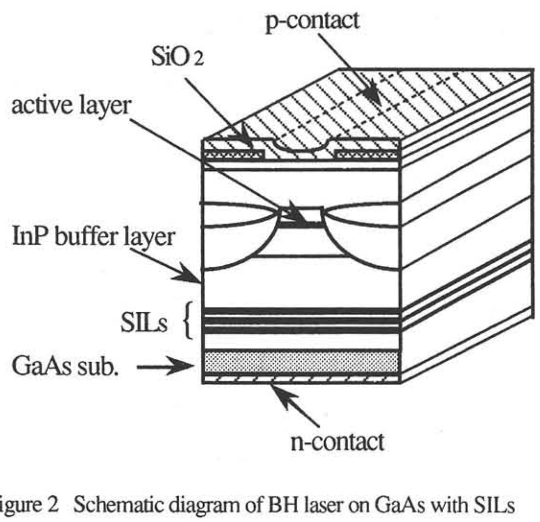

Figure 2 Schematic diagram of BH laser on GaAs with SILs

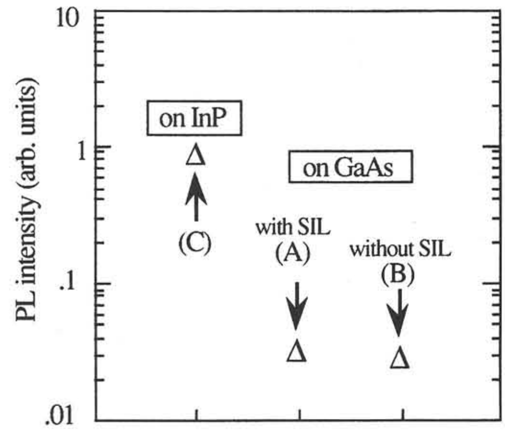

Figure 3 PL intensity of laser active layers

EPD at the top surface from $6x10^7$ to $3x10^7$ cm^{-2}.

Then (i) a 2 μm n-InP cladding layer, (ii) a 0.14 μm undoped InGaAsP (λ = 1.3 μm) active layer and (iii) a 0.4 μm p-InP cladding layer were grown. The mesa structure was formed by wet etching and its exposed region was buried with (iv) 2 μm p-InP and (v) 1 μm n-InP current blocking layers. The stripe width was 1.4 μm. Finally (vi) a 2 μm p-InP layer and (vii) a 0.3 μm p-InGaAsP contact layer were grown. For comparison, we made another laser on GaAs with the same structure as (A) except with no SILs (B), and an identical BH laser on an n-InP substrate (C). Figure 3 shows the PL intensity from the active layer of these three lasers. The luminescence from (A) and (B) is much weaker than that from (C). Comparing the two GaAs lasers, the luminescence from (A) is slightly stronger than that from (B). These facts indicate that the SIL reduces the dislocation density of the active layer, but the density is still much higher than that on InP.

Figure 4 shows the effect of the SIL on device performance very clearly. It illustrates the distribution

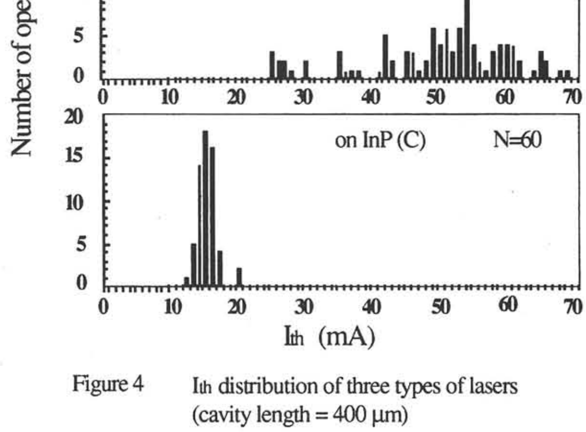

Figure 4 Ith distribution of three types of lasers (cavity length = 400 μm)

Table 1 Laser characteristics derived from the following equations;

$$\eta_d^{-1} = \eta_i^{-1} \left(1 + \frac{\alpha}{\ln R^{-1}} L \right)$$

$$J_{th} = J_0 d + \frac{d}{\beta \Gamma} \left(\alpha + \ln R^{-1} \frac{1}{L} \right)$$

where

$d = 0.14\ \mu m$, $R = 0.3$, $\Gamma = 0.25$

	on GaAs (A)	on GaAs (B)	on InP (C)
η_i (%)	76	75	76
α (cm^{-1})	13.1	15.1	10.7
β (cm^2/A)	0.9×10^{-6}	0.6×10^{-6}	1.4×10^{-6}
J_0 (A/cm^3)	2.9×10^8	3.4×10^8	6.7×10^7

of threshold current (I_{th}) of 100 laser chips each of (A) and (B), and 60 chips of (C) under pulse operation at room temperature. The cavity length is 400 μm. The average I_{th} of (A) is 34 mA, though that of (B) is 50 mA. This 30 % reduction in I_{th} was caused by the dislocation reduction due to the SIL. Moreover, the I_{th} of (A) are dispersed within a smaller range than that for (B). This indicates that the dislocation distribution in the active region is more uniform for (A) than (B). This fact can also be attributed to the SIL, i.e. the strain field at the SIL/InP interface not only bends dislocations but also scatters dislocations uniformly. TCA may also promote these phenomena because if dislocations are activated enough to move, the SIL can act on them again.

The external differential quantum effeiciency (η_d) and threshold current density (J_{th}) were investigated varying the cavity length (L). The internal differential quantum efficiency (η_i), internal loss (α), gain coefficient (β) and transparency current density (J_0) are summarized in Table 1. Most of the values are better for

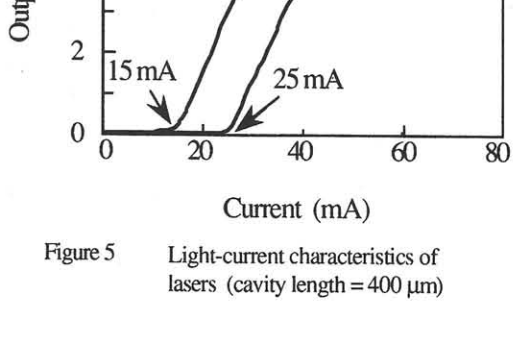

Figure 5 Light-current characteristics of lasers (cavity length = 400 μm)

(A) than (B). This is also due to the SIL reducing dislocations. However (A) is still poor than (C) especially in β and J_0, because (A) has a much higher dislocation density as shown in Figure 3.

Figure 5 shows the light-current characteristics under cw operation at room temperature. The cavity length is 400 μm. I_{th} and the slope efficiency were the same as those under pulse operation. The minimum I_{th} of both lasers on GaAs is the same at 25 mA, and their slope efficiency is about 0.26 W/A. They operated more than 100 hours continuously at room temperature.

5. CONCLUSION

We have investigated the reduction of threading dislocations by InGaP SIL in InP/GaAs, and examined its effect on device performance. Observation of the dislocation structure by cross-sectional TEM showed the SILs ability to bend dislocations. BH lasers with a wavelength of 1.3 μm were fabricated on a GaAs substrate employing the most suitable SIL. Their characteristics such as I_{th}, α, β and J_0 were measured, and found to be improved by SIL insertion. This fact indicates that SIL should work effective in device fabrication on lattice-mismatched substrate.

ACKNOWLEDGEMENTS

The authors would like to show their gratitude to Dr. D. J. Olego of Philips Labs. for technical advice on this work, and Dr. H. Kakibayashi of Hitachi Central Research Labs. and Dr. M. Tamura of the Optoelectronics Technology Research Labs. for the measurements and helpful discussion regarding the TEM observations.

REFERENCES

1) D. Deppe, D. W. Nam, N. Holonyak, Jr., K. C. Hsieh, R. J. Matyi, H. Schichijo, J. E. Epler, and H. F. Chung: Appl. Phys. Lett. **51** (1987) 637

2) M. Razeghi, M. Defour, R. Blondeau, F. Omnes, P. Maurel, O. Acher, F. Brillouet, J. C. C. Fan, and J. Salerno: Appl. Phys. Lett. **53** (1988) 2389

3) M. Sugo, H. Mori, Y. Sakai, and Y. Itoh: Appl. Phys. Lett. **60** (1992) 472

4) T. Kimura, T. Kimura, E. Ishimura, F. Uesugi, M. Tsugami, K. Mizuguchi, and T. Murotani: J. Crystal Growth **107** (1991) 827

5) Y. Watanabe, Y. Kadoya, H. Okamoto, M. Seki, and Y. Ohmachi: J. Crystal Growth **93** (1988) 459

6) N. Hayafuji, S. Ochi, M. Miyashita, M. Tsugami, T. Murotani, and A. Kawagishi: J. Crystal Growth **93** (1988) 494

7) T. Soga, Y. Kohama, K. Uchida, M. Tajima, T. Jimbo, and M. Umeno: J. Crystal Growth **93** (1988) 499

8) A. Seki, F. Konushi, J. Kudo, and M. Koba: J. Crystal Growth **93** (1988) 527

9) T. Soga, T. Jimbo, and M. Umeno: Appl. Phys. Lett. **56** (1990) 1433

10) A. Hashimoto, N. Sugiyama, and M. Tamura: Jpn. J. Appl. Phys. **30** (1991) L447

11) H. Kakibayashi and F. Nagata: Jpn. J. Appl. Phys. **25** (1986) 1644

12) J. W. Matthews and A. E. Blakeslee: J. Crystal Growth **27** (1974) 118